Peak Torque Calculations for Backstops in Conveyors

Dr. Ing. Timtner
Executive President of RINGSPANN GmbH, Bad Homburg, Germany

1. Introduction

Conveyor plants of all types are an important part of the infrastructure all over the world. Continuous conveyors represent an essential part of conveyor plants.Today the largest plants reach a conveyor length of many kilometres with a bulk stream up to 40,000 t/h and a conveyor height of many hundred metres, [1] and [3].

Apart from the horizontal conveyance of material continuous conveyors are often used in order to over-come height differences. lt is, however, important to take certain safety measures with such inclined conveyors: In case of drive failure, a reversal of the continuous conveyor - caused by the weight of the conveyed material - must be prevented. This is the function of backstops. They are fully automatic and prevent the downward movement of the conveyor belt, i.e. , they prevent the rotation of the input shaft.

Although very many backstops exist for these applications, it is still difficult to determine their safe ope-ration in advance. Mistakes are common especially with big units, leading to breakdowns and serious damage. Some common calculation methods use the motor power under normal conveyor conditions as a basis for calculation. The physical system in operation under normal conditions is, however, different from that occurring in the case of reverse movement of the inclined conveyor plant.

This paper introduces a new method of calculation, which uses the physical system in effect during the stopping process. lt especially takes into consideration the non-linear torque between the conveyor plant and the backstop. The load sharing in a multiple drive system with several backstops is also analyzed.

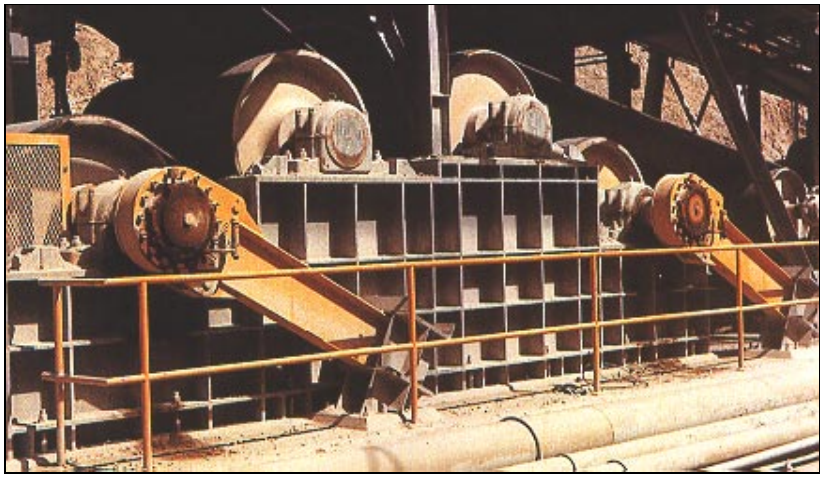

Fig.1 Two low speed backstops on the primary and secondary drive of a conveyor, La Caridad Mine, Mexico (MARLAND, La Grange)

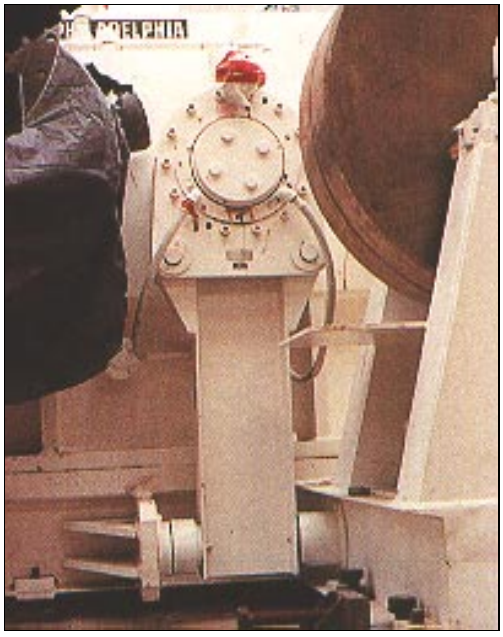

Fig.2: High sped backstop on the intermediate shaft of a conveyor gear (MARLAND-RINGSPANN, La Grange)

2. Location and Designs of Backstops

Depending on the size of the conveyor plant, the backstopping units are located in various positions. In small and medium-sized units, it is common practice to place the backstops directly at the electric motor, the gear motor or the gear reducer. In large conveyor plants, big backstops have very often been placed directly on the conveyor pulley shaft between the bearings and the output shaft of the gear reducer, sometimes on both sides. In the case of multiple drives, backstops are often located at each input shaft (Fig. 1). In recent years, particularly on the initiative of European manufacturers, this type of construction has been discontinued because of the high costs involved in this large size of backstop, so that many companies now install the backstops on input or intermediate gear-shafts. Such backstops are considerably smaller than earlier ones (see Fig. 2). For the advantages and disadvantages of both types see [7] and [8].

More comprehensive information about the location and design of backstops is given in [5]. Here, as in [7] and [8], the various types for higher speeds are also shown. In order to remain free of wear, it is a basic requirement of such backstops that they have centrifugal lift-off during normal operation. This can only be achieved by using sprag type freewheels. One type of freewheel that has proven itself in this field is one in which the inner ring with a sprag cage is located on a gearshaft end and the outer ring is bolted to the gear housing. During normal operation the shaft rotates and the sprags rotate without contact with the stationary outer ring.

3. Former Calculation and Selection Methods

References [4], [5], [7] and [8] reveal that various procedures exist for establishing the correct back-stop. One example given here is the CEMA method (Conveyor Equipment Manufacturers' Association). In this case, the torque is calculated from the conveying power minus half the friction power, using a safety factor of 1.5. Some formulas use the nominal motor power, while others rely on the stall torque of the electric motor. None of these criteria enable more than rough approximations and make virtually no allowance for the physical behaviour of the system as a whole whenever the conveyor belt is stopped by the backstop operation. This process results in a state of damped vibration which is subject to the influence of different spring stiffnesses, masses and damping. As is shown in [8], extreme torques can occur during braking which can be between 4 and 10 times higher than the normal input torque or the nominal motor torque. Particularly high torques occur in a system with non-linear torsional spring curves. These can occur as a result of torsionally flexible couplings with rubber elements, gear tooth clearance, or through the wind-up curve of the backstop itself.

Several decades of practical experience and scientific research have shown that the method demon-strated in [8] is the most reliable for approximate selections. It was developed with the assistance of well-known gear manufacturers. According to this formula, the backstop to be selected should have a maximum torque *M,* where

$$M \geq 3{,}5 \cdot \eta_{ab}^{2} \cdot M_A \qquad (1)$$

In this case, M_A, consists of the torque required to overcome friction resistance and the torque required to raise the conveyed materials. The factor of 3.5 is a dynamic factor which takes into account all the above-mentioned dynamic characteristics of the plant, while η_{ab} is the conveyor plant's officiency (= lifting horse- power divided by input horsepower). For further details, refer to [8] and [5] (RINGSPANN GmbH). This method does not take into consideration the specific conditions of the particular installation.

4. Calculation Procedure for Dynamic Peak Torques for Backstops in Conveyor Belts

4.1 Preliminary Remarks

One of the main objectives in the development of this new calculation procedure was to establish the dynamic peak torques in conveyor plants by the simplest analytical method possible. It was most important that the calculation should be feasible on the basis of the specific data normally available. Moreover, the procedure was supposed to show how the specific change of variable parameters influences the peak torques. While extensive and highly efficient computer simulation programmes for dynamic structures are available, they frequently require an unnecessarily high data input and the mechanical model used is often difficult to grasp.

Most of the major computer programmes for conveyor plant calculations which take into account the entire dynamics (see [3], for example) are designed on the basis of normal operating procedures and the starting and stopping periods. As far as the author is aware, no dynamic calculations in these computer simulation programmes have taken the backstop into account correctly. The calculation procedure developed under the above-mentioned conditions will be described in more detail later.

4.2 Idealization of the Real System onto the Mechanical Simplified System

Fig. 3 is a schematic diagram of a large conveyor system with three drive units. In this case, two of the units are connected to the main pulley (head pulley) and the third to the secondary pulley. The head pulley is shown again in enlarged form in Fig. 4. Here one can see that the pulley is driven by two electric motors, each with a two-stage gear system. Between the gear and the pulley there is a torsionally flexible coupling. The backstop is attached at the intermediate gear shaft. The belt elasticity between the head drum and the tail pulley is presumed here to be very large in comparison to other elasticities.

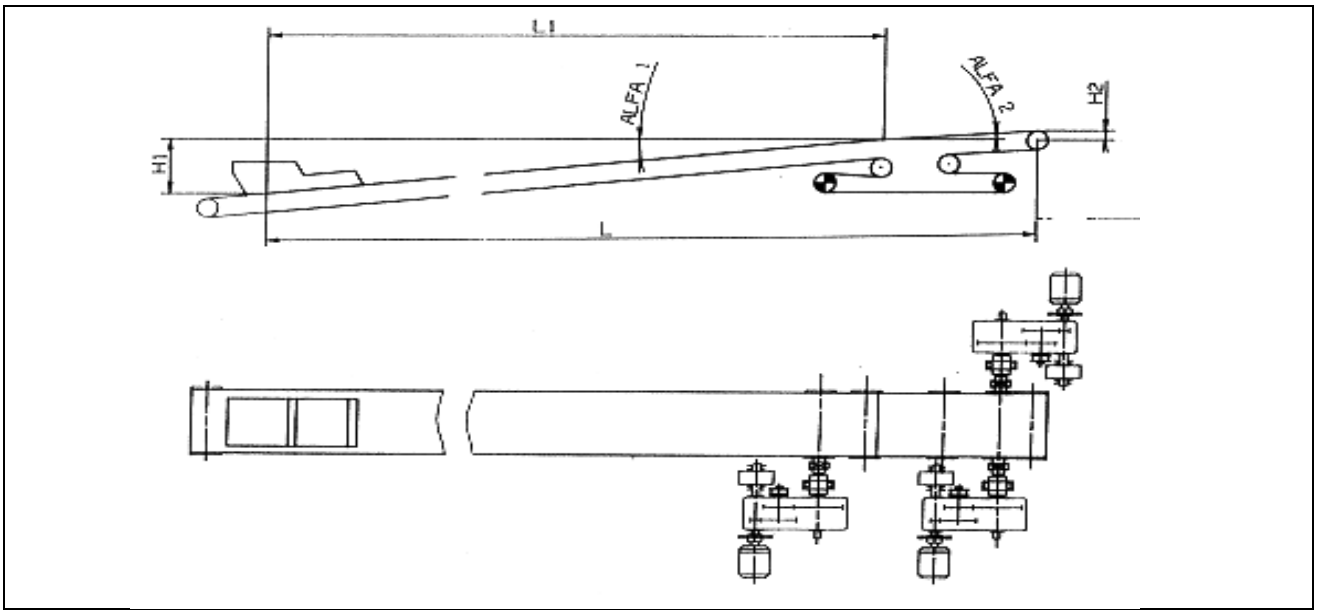

Fig.3: Inclined conveyor drive arrangement

As required in Section 4.1, the system is now reduced to a one mass torsion oscillator. The initial presumption is that in all cases both gear units, and therefore the two backstops as well, are under equal load. If all torsional stiffnesses and masses are now transferred to the backstop shaft, the result is as shown in Fig. 5. The greatest degree of simplification has been made in the lower half of the picture. In the middle of the lower half one can see that all masses are concentrated in the conveyor mass *m*, which lies to the left of the coupling. On the right there only remains the backstop, which in the case of operation has the torque stiffness $\hat{c}_{FG}$. A frictional force F_R is applied to the conveyor mass and acts in the opposite direction to the conveyor velocity. The extremely simplified system

diagram is visible in the lower right half of the picture, and will be used as the basis for further explanation.

The simplified diagram from Fig. 5 appears on the left in Fig. 6a. It shows a normal conveying operation in a stationary situation. Force F pulls the mass m by means of the entire reduced spring stiffness c_1 at a velocity of $\dot{x}$ in an upward direction. The frictional resistance is F_R.

Fig.4: Two gear drives on a head pulley of the conveyor of Fig. 3

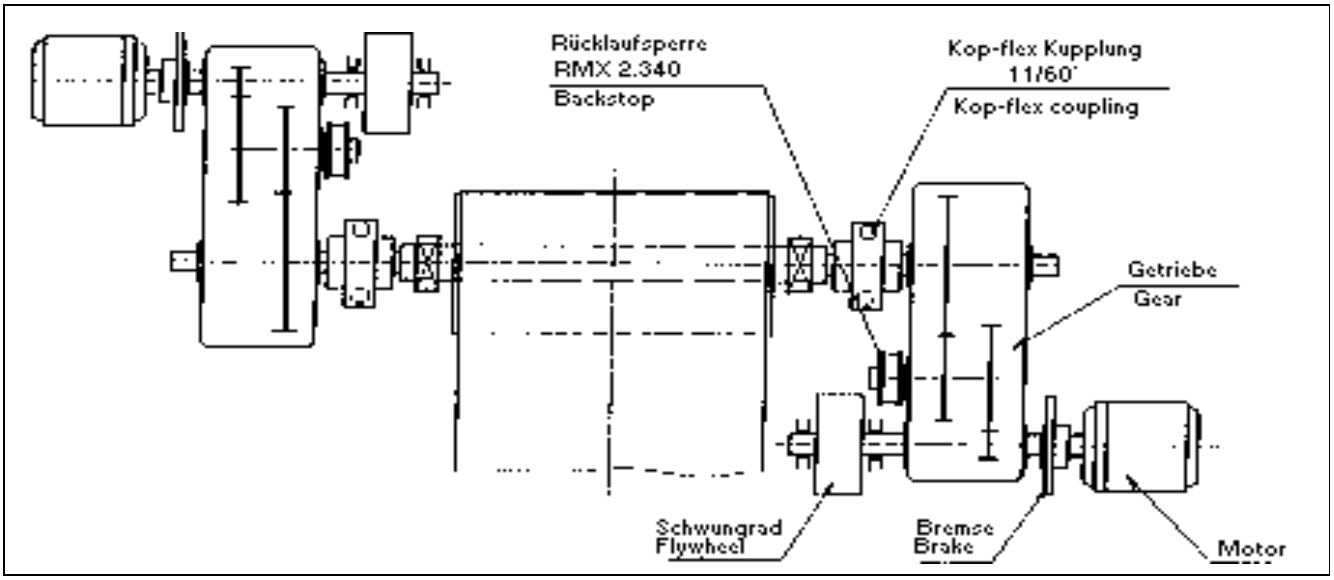

Fig.5: Belt drive and mechanical model of the drive arrangement.

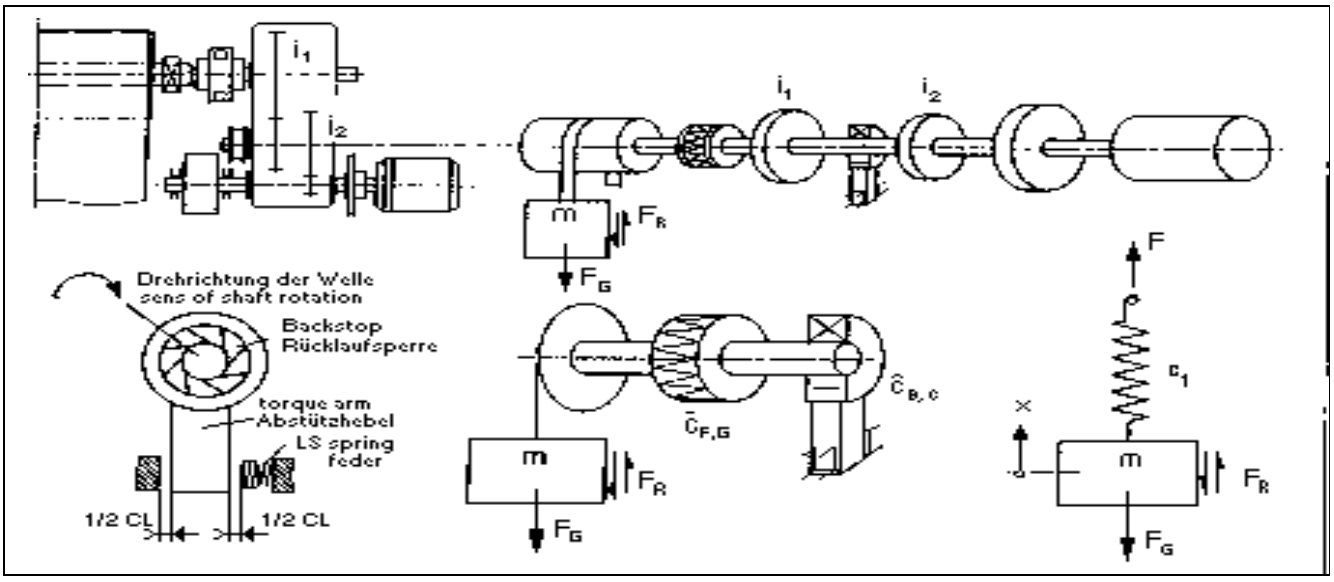

Fig. 6b shows the complete system shortly after a sudden loss of power transmission. The spring c_1 is relaxed, but the mass m, because of its inertia, still has a velocity of $\dot{x}$. Forces F_G and F_R are still in action.

Fig. 6c shows the situation once the speed has been reduced to zero and the conveyor belt ceases moving. It is important to realise that, because of the backstop's function, a different spring-mass system comes into effect at this moment. The original spring stiffness c_1 is combined with the torsional spring stiffness of the backstop c_2 so that a new total spring stiffness c_{ges} is created.

Fig.6: Mechanical models for the conveyor drive and different situations

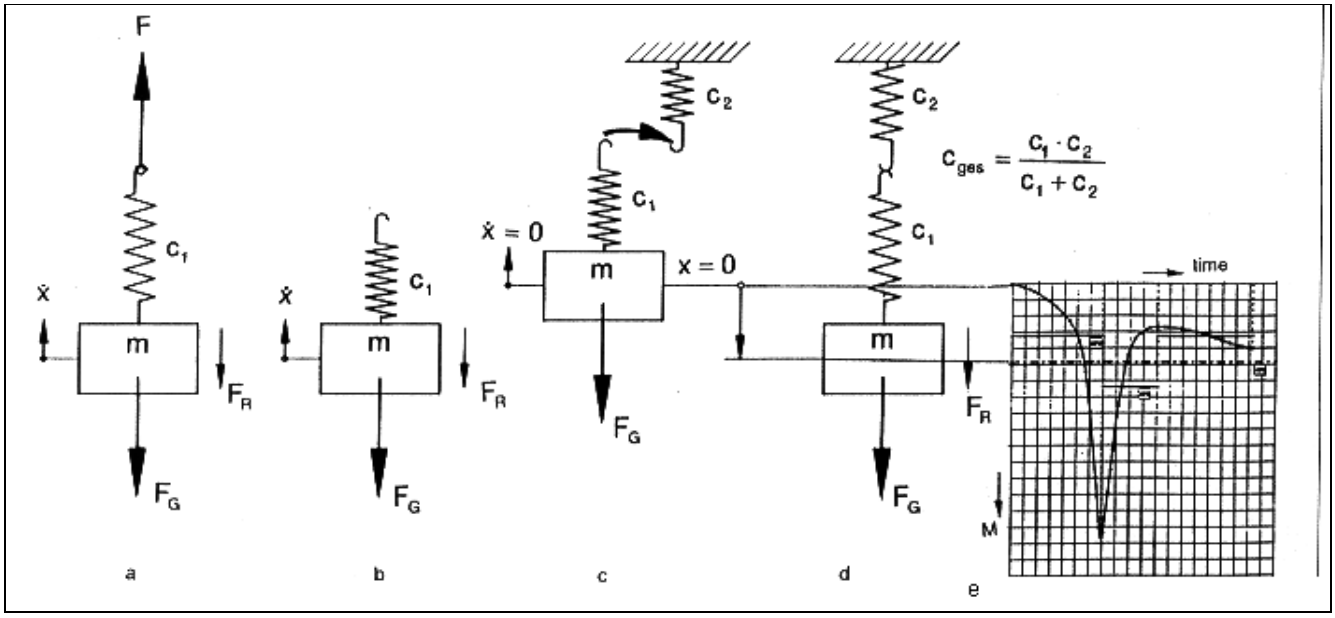

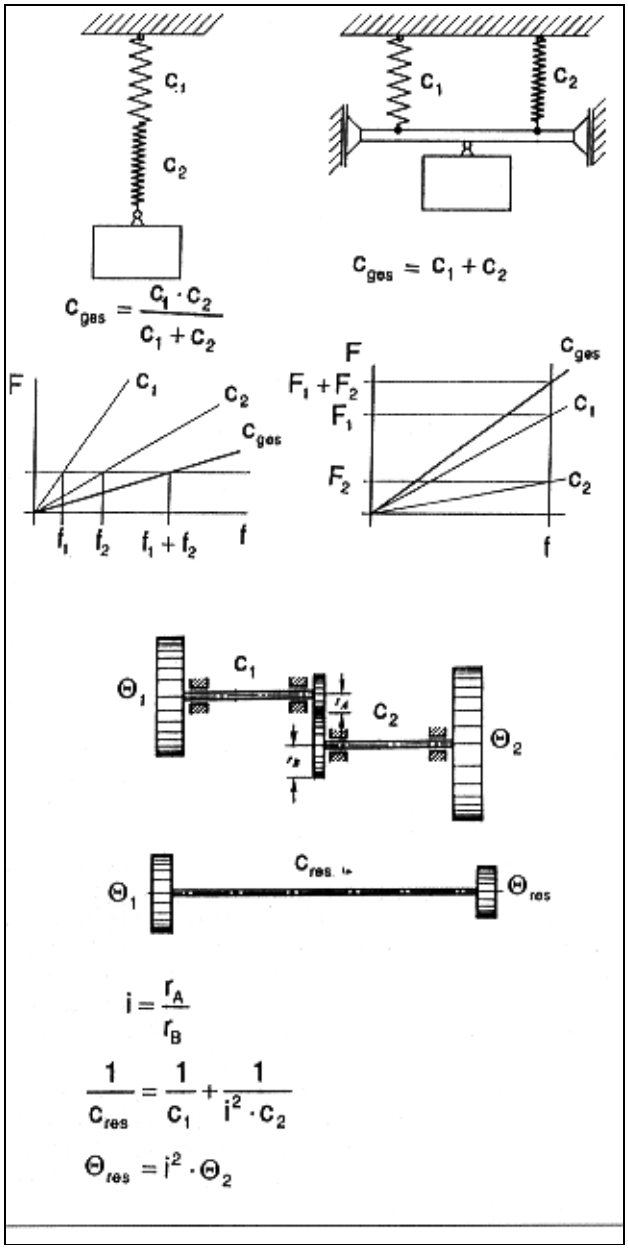

Fig.7: Spring rate combination and inertia reductions

This state is shown in Fig. 6d at the point where the mass, as a result of the spring stiffness c_{ges}, would have achieved its new static idle position. Given an undamped vibration, the mass would move around this static idle position.

Fig. 6e, referring to later results, shows the oscillations in the model system for a non-linear spring curve and intense frictional damping. It is obvious that this diagram shows a very damped vibration with only one peak.

For further information on the reduction of the different torsional masses and torsional spring stiffnesses and the combination of springs in parallel or series systems, see [10 and 11]. Here it is particularly important that during the reduction of masses from a slower to a faster-moving shaft, the masses are reduced at a ratio of i^2, while the spring stiffnesses increase at a rate of i^2 (see Fig. 7). This often leads to very surprising results; for example, the high speed rotating motormass often has considerably more stored energy than all other masses in motion.

Fig. 7 shows the situation for linear spring curves. In a non-linear case, two or more spring curves would be combined. In series systems the spring travel (torsional angles) add up for every force (torque); in parallel systems, the forces (torques) add up for every spring travel (torsional angle).

4.3 Differential Equation for the Mechanical Simplified System

If the mechanical simplified system according to Fig. 6 was a linear oscillator with the spring stiffness c_{ges} of inertia moment without the frictional damping F_R the differential equation for the torsional oscillation would be as follows:

$$\theta \cdot \ddot{\varphi} + \hat{c} \cdot \varphi = 0 \qquad (2)$$

Taking into account the parameters, the solution of this differential equation according to [10] or [11] is $x = 0$ and $\dot{x} = 0$ for $t = 0$:

$$\varphi(t) = \frac{g}{\omega^2}(1 - \cos \omega t) \qquad (3)$$

$$\omega^2 = \frac{\hat{c}}{\theta} \qquad (4)$$

Because in a linear case the torque is proportional to the torsional angle with the proportionality factor $\hat{c}$, the torque, depending on the time necessary for this linear oscillation, is as follows:

$$M(t) = \frac{\hat{c} \cdot g}{\omega^2}(1 - \cos \omega t) \qquad (5)$$

It is obvious from this formula that after a half-oscillation for $\omega \cdot t = \pi$, the dynamic torque has double the value of the static torque given by the mass at rest. This is explained very clearly in [8].

If the reduced spring stiffness no longer constitutes a linear function between torsional angle and torque, but is non-linear and has the same effect on the conveyor system as the frictional damping, the differential equation is as follows:

$$\theta \cdot \ddot{\varphi} + R(\varphi) + (\operatorname{sgn} \dot{\varphi}) \cdot S = 0 \qquad (6)$$

The term $(\operatorname{sgn} \dot{\varphi}) \cdot S$ represents the frictional damping with the constant torque S, while (sgn $\dot{\varphi}$) takes into account the torque direction in opposition to the direction of the speed $\dot{\varphi}$.

The function $R(\varphi)$ represents the non-linear torsional spring characteristic of the entire system. In the example under discussion we are dealing in almost all cases with progressive torsionalspring curves, as in Fig. 8. The form of these curves is determined by rubber elastic elements in flexible couplings, but the charactoristics of freewheels (see [6]) are also progressive. It has been proved that such curves can be very simply described by the following equation:

$$M(\varphi) = A \cdot \varphi + B \cdot \varphi^n \qquad (7)$$

With actual figures the following two formulas for curves *B* and *G* emerge in Fig. 15:

$$M_B(\varphi) = 7{,}31 \cdot 10^5 \cdot \varphi + 6{,}92 \cdot 10^{10} \cdot \varphi^5 \qquad (8)$$

$$M_G(\varphi) = 2{,}87 \cdot 10^5 \cdot \varphi + 4{,}90 \cdot 10^{12} \cdot \varphi^9 \qquad (9)$$

The fully extended curves in Fig. 8 have been calculated using the above formulas; the crosses along the curves show the real wind-up curves. *B* is the wind-up curve of the backstop; *G* is the total wind-up curve, including the torsionally elastic coupling and an initial backlash at the torque arm of the backstop. Because of the low gradient for small torsional angles, such backlashes as well as tooth clearance in the gears can be taken into consideration when calculating the wind-up curves. It should also be mentioned that the exponent of φ in the second equation for the backstop only equals 5,

whereas in Eq. 9 it equals 9. So the progressive form of the wind-up curve is more evident in the total system than it is for the backstop alone. This fact has a negative influence on the dynamic peak torques.

The movement in the backstop condition starts at the time *t = 0* with $\varphi = 0$, and the movement starts - as mentioned above - around the static idle position.

The corresponding torsional angle φ_o . depends solely on the mass m and the wind-up curve. lt results from the following formula:

$$(\varphi_o - \varphi_L \cdot m(\varphi_o) - \int_{\varphi_L}^{\varphi_O} m(\varphi) d\varphi =$$

$$= -(\varphi_R - \varphi_o) \cdot m(\varphi_o) + \int_{\varphi_O}^{\varphi_R} m(\varphi) d\varphi \qquad (10)$$

In this formula, some standardizations and simplifications have already been made. Using Eq. (7) we get:

$$0 = (\varphi_R - \varphi_L)\left(\varphi_o + \frac{B}{A}\varphi_o^n\right) -$$

$$- \left[\frac{1}{2}(\varphi_R^2 - \varphi_L^2) + \frac{B}{A(n+1)}(\varphi_R^{n+1} - \varphi_L^{n+1})\right] \qquad (11)$$

Using this formula, the angle of the static idle position (p. can now be calculated.

lf we introduce into Eq. (6), as in the linear case Eq. (4), the theoretical natural frequency

$$\mathrm{K} = \sqrt{\frac{A}{\Theta_{red}}} \qquad (12)$$

as well as

$$\overline{\varphi} = \varphi - \varphi_a \qquad (13)$$

the differential equation of Eq. (6) now appears as follows:

$$\ddot{\overline{\varphi}} + \mathrm{K}^2\left[m(\overline{\varphi}) + (\operatorname{sgn}\dot{\overline{\varphi}}) \cdot s\right] = 0 \qquad (14)$$

The solution of this non-linear differential equation cannot be found by one simple formula for such extremely non-linear functions as shown in [10], but there exists a number of approximation procedures. As indicated in Section 4.1, the author has decided to proceed as analytically as possible in accordance with [10]. Thus, for the vibration process we do not get a solution for the torsional angle dependent on the time, as in the linear case, but rather a solution of time dependent on the torsional angle:

$$t(\overline{\varphi}) = \frac{1}{\sqrt{2} \cdot \mathrm{K}} \int_o^{\varphi} \frac{d\overline{\varphi}}{\sqrt{\Im(\varnothing) - \Im(\overline{\varphi})}} \qquad (15)$$

lt is not necessary to show the intermediate calculations here. After the corresponding integrations have been made, we get the following formula for the calculation of the time function with regard to the torsional spring curves according to Eq. (7):

$$t(\overline{\varphi}) = \frac{1}{K}\int_{o}^{\varphi} \frac{d\overline{\varphi}}{\sqrt{(\overline{\varnothing}^2 - \overline{\varphi}^2) + 2\cdot\frac{B}{A}\left[\frac{(\varphi_o + \varnothing)^{n+1}}{n+1} - \varphi_o^{n+1}(\overline{\varnothing} - \overline{\varphi})\right]}} \qquad (16)$$

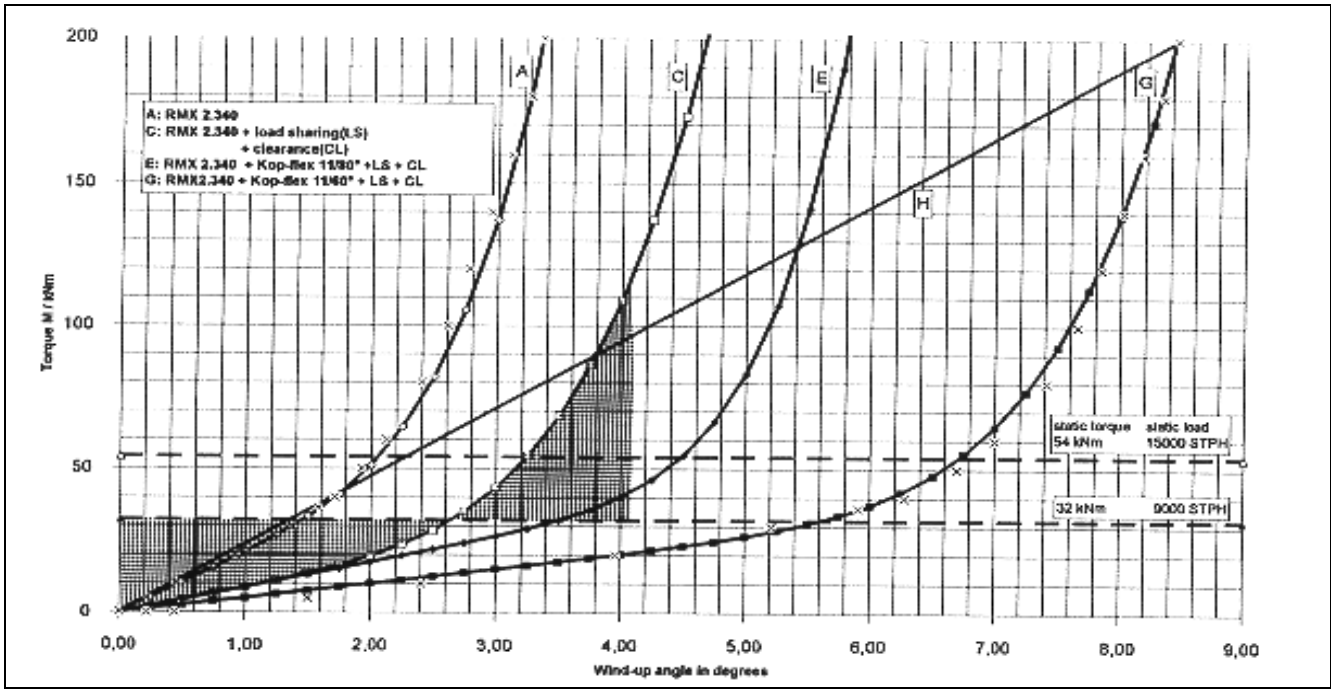

Fig.8: Wind-up characteristics in a conveyor drive at the backstop shaft.

As can be easily seen, the reduced moment of inertia, the spring stiffnesses and also the friction damping are all included in the constants *A* and *B,* and the integral in Eq. (16) can be calculated. For this calculation a program with three small sub-routines has been developed using a Hewlett Packard calculator HP42S, in which the functions Solver and ∫ *f(x)* have been used repeatedly in suitable ways. After the input of the necessary constants the first quarter oscillation in the slowing-down process, which alone is important, can be calculated in less than 20 seconds. It is then very easy to carry out and calculate parameter modifications. The calculation of the peak torque takes only 5 seconds.

In accordance with the formulas above, we get a certain time for a previously chosen torsional angle. The corresponding torque at the backstop can easily be assigned by the calculation from the torsional angle. Thus the function "torque in relation to time" can be easily shown.

A simple test method for the calculation process described above is the use of a linear curve with a previously known complete method of solution. Both the calculation with the numerical method explained above and the complete method of solution must yield the same torque curve.

Fig. 8 shows such a curve indicated by H. In Fig. 9 the torque and course of time have been calculated for the described conveyor plant and torsional spring curve for two load conditions. In order to simplify the calculation it has been assumed that there is no friction damping. The result for the two load conditions of 9,000 STPH and 15,000 STPH (STPH = short tons per hour) was a peak torque at the backstop of 64.6 kNm and 108 kNm with torques in the static idle position of 32.2 and 54 kNm respectively, in other words they showed exactly half the peak torque, as could have been expected. The crosses in Fig. 9 during the first quarter-oscillation show clearly what the complete calculation method with *cos x · t* produced. In this area the deviations are visible, but very small. For longer periods of time the results coincide fully with the numerical calculation. The calculation method has also been examined for two cases with real, non-linear torsional spring curves in a backstop bench test. The results were surprisingly identical.

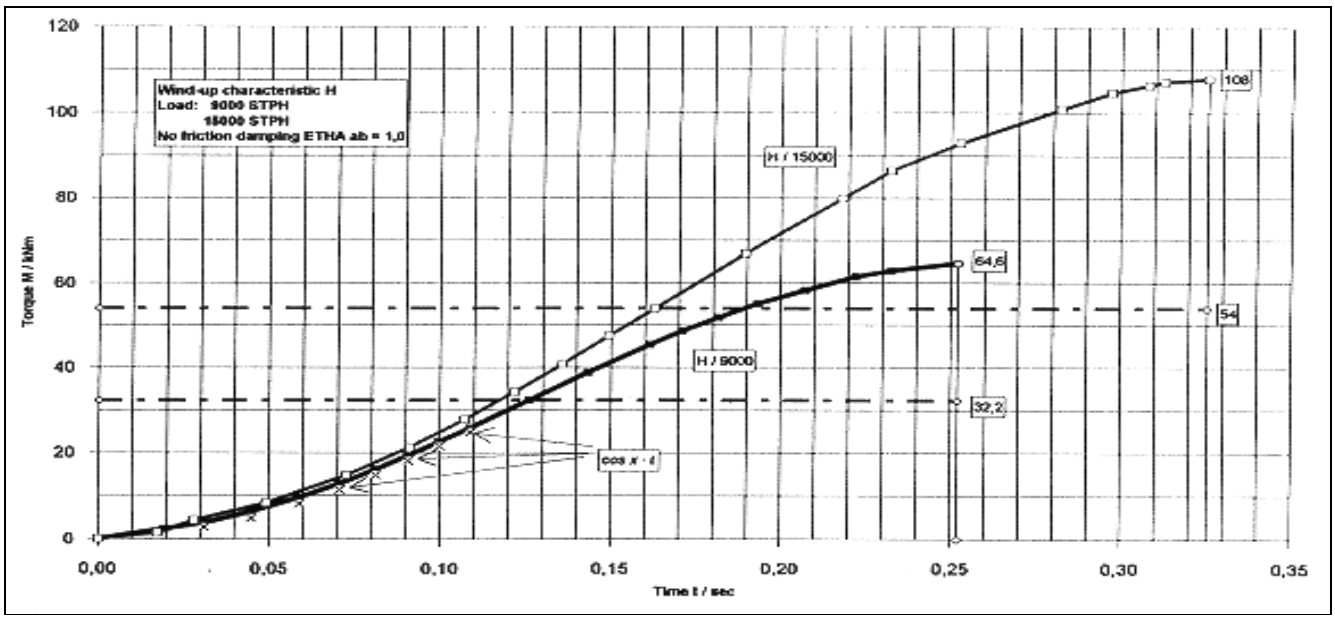

Fig.9: Dynamic torque vs. time, first half backstopping cycle at the backstop shaft.

5. Calculation Results for Inclined Conveyor Plant with Identical Load Distribution at Two Backstops

5.1. Construction of the Conveyor Plant and Configuration of Power Transmission Units

The calculation method described in Section 4 was used for an existing inclined conveyor plant similar to that in Fig. 3, with varying parameters, in order to determine the peak torques in the backstops. lt was also to be determined what maximum overload of the conveyor belt was capable of without destroying the backstops.

The static reverse torque on the backstop shaft can be determined by the following formula:

$$M_{To} = \frac{g}{i} \cdot \frac{D}{2} \cdot L^{\bullet} \cdot G \cdot (\sin\alpha - K \cdot \cos\alpha) \qquad (17)$$

where:

g	acceleration due to gravity (9.81 M/S2), [M/S2]
i	transmission ratio from pulley to backstop
D	pulley diameter, [ml
$L^{\bullet}$	constant, [kg/STPHI
G	conveyor belt load, [STPH]
φ	angle of inclination of the conveyor, or substitute angle in the case of different inclinations [o]
K	constant with regard to friction damping.

The constant *K* includes the "downwards"- efficiency llab according to the following formula:

$$\eta_{ab} = 1 - \frac{M_R}{M_L} = 1 - \frac{K}{\tan\alpha} \qquad (18)$$

As Fig. 3 shows, the conveyor plant had three drives. Each gear unit was equipped with its own backstop. We have to assume, however, that in accordance with Fig. 4 only the two backstops at the

head pulley were effective. Because of the flexibility of the belt the backstop on the third drive at the secondary pulley could not be expected to take any significant load. The calculations in this section are based on the assumption that both backstops at the head pulley are equally loaded.

Furthermore, it was assumed for the backstops that at the beginning of the backstop condition there was the maximum amount of (CL) clearance, and that the load sharing springs were acting, so that both facts generated a smoother torsional spring curve at the backstop (see Fig. 5).

The main data of the conveyor plant are as follows:

conveyor length *L*	1,080 m
total conveyor height *H*	101 m
nominal capacity of one electrical motor	1,270 kW
total ratio	*i* = 18.9
maximum torque of one backstop	200,000 Nm.

5.2 Torsional Spring Characteristics of the Individual Elements and Reduction on the Backstop Shaft

Fig. 8 shows the four wind-up curves *A, C, E* and *G, A* is the original wind-up curve of the backstop, in this case an RMX 2.340. *C* shows the curve of the backstop including the load share device and the clearance at the torque arm of the backstop (Fig. 5). As can be seen, this creates a maximum torsional angle at a torque of 200 kNm of 4.60, compared to the torsional angle of the backstop alone of less than 3.40. *G* is the total system wind-up curve as seen at the backstop shaft. This curve includes the characteristics of the torsionally flexible coupling (Kop-flex coupling L/60°). Here the gear ratio between the conveyor pulley and the backstop operates in the squared dimension, as explained in Section 4. The torsional angle at 200 kNm is 8.4°. Finally, *E* is the wind-up curve with a much stiffer, rubber-elastic coupling (Kop-flex coupling L/80°). In this wind-up diagram, the static idle positions for the two loads 9,000 STPH and 15,000 STPH are shown. They result from torques of 32 kNm and 54 kNm respectively. The corresponding angles can be determined from the different curves. Shading has been used with curve *C* to indicate how an energy balance has emerged above and below the point of equilibrium. One can see that because of the equality in area in the progressive curve, the maximum torque in the case of an undamped vibration must be approximately 120 kNm, in other words, when compared with the static torque of 32 kNm and if the torsionally elastic coupling did not exist, a dynamic factor of four would result.

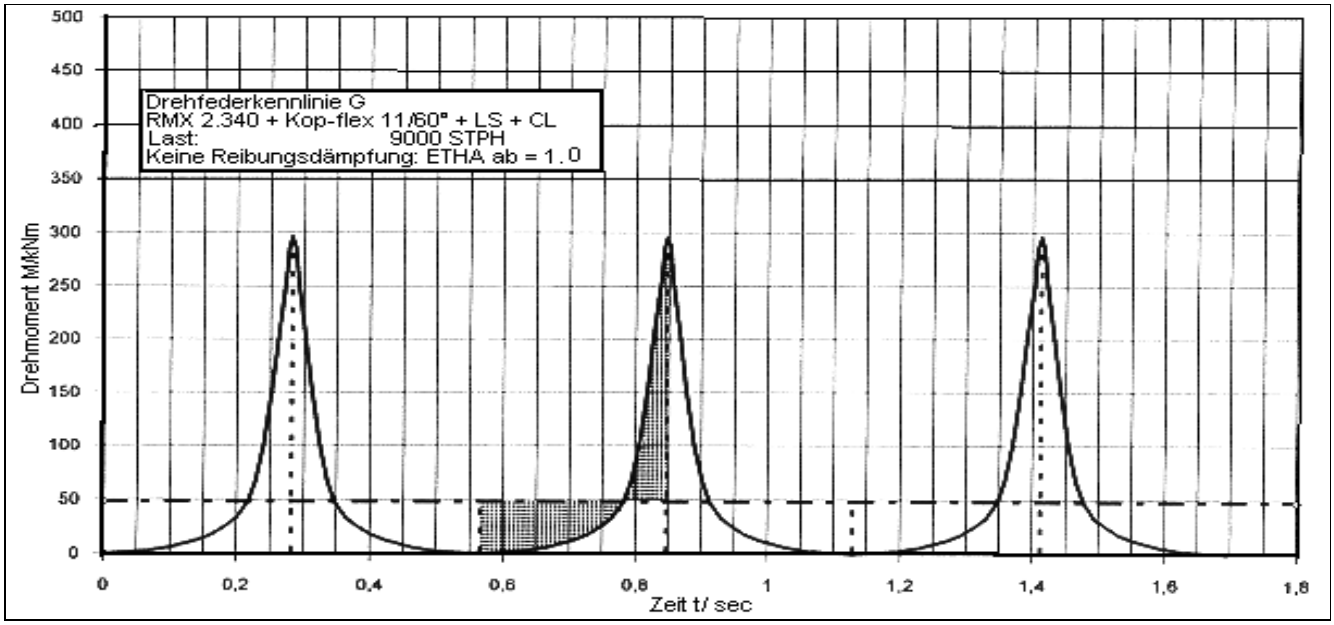

Fig.10: Dynamic torque vs. tme, ful backstopping cycle at the backstop shaft.

5.3 Torque-Time-Functions

The calculation procedure is now begun, using the wind-up curves outlined above. Fig. 10 shows the oscillation pattern which would occur without damping. This oscillation pattern occurs when the belt is halted with a load of 9,000 STPH utilizing wind-up curve *G*. In this case there is a peak torque in the backstop of 300 kNm, i.e., six times the static torque of 50 kNm. In the case of the second oscillation, the areas above and below the static idle position in this diagram are also shaded.

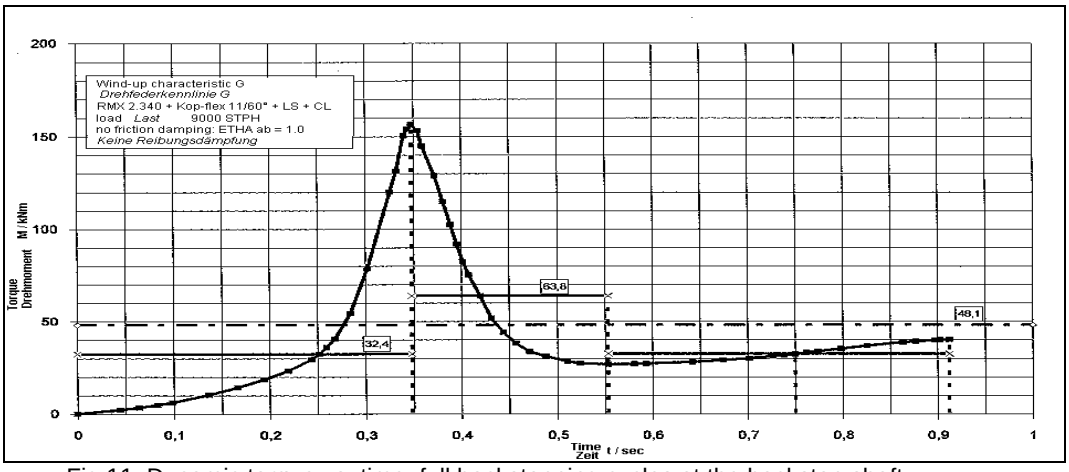

Fig.11: Dynamic torque vs. time, full backstopping cycles at the backstop shaft.

Because this is a torque-time function, the shaded areas represent the rate of torsional impulse, and as we are dealing here with an undamped oscillation, both areas must be of the same value because of the consistency of the torsional impulse. This was confirmed by planimetry.

Fig. 11 shows for curve *G* the torque curve in relation to time under real conditions with friction. On the basis of past experience a degree of frictional activity to the value of η_{ab} = 0,6733 was chosen. The static idle positions (including the constant force of damping) can be seen in the figure; they are 32.4 kNm for maximum wind-up (reverse running) and 63.8 kNm for minimum wind-up torque (forward running). The static mean is 48.1 kNm. Under the conditions described above, the entire stopping process would last somewhat more than 0.9 sec, a realistic figure.

As one can see from this diagram, when determining the peak values for the backstop it is quite sufficient to examine the first half-oscillation alone. No higher peak value can occur at a later stage.
For this reason, only the initial half-oscillations are shown in Fig. 12 for the torsional spring curves *A* and *G* with respective loads of 9,000 and 15,000 STPH. For curves *C* and *E*, only the peak torques at the end of the first half-oscillation have been indicated by means of black squares or triangles. This diagram makes very clear the extent to which the maximum torque depends on the load. With a linear curve, the peak torque would always have to be double the static torque. In case of a progressive characteristic the peak torque rises disproportionally.

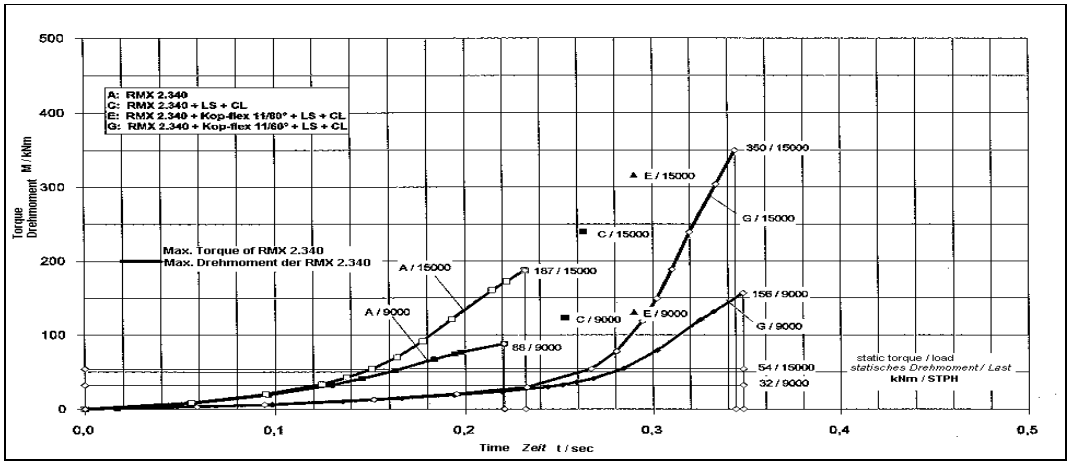

Fig.12: Dynamic torque vs. time, first half cycle

Fig.13: Dynamic peak torque vs. load, first half cycle first

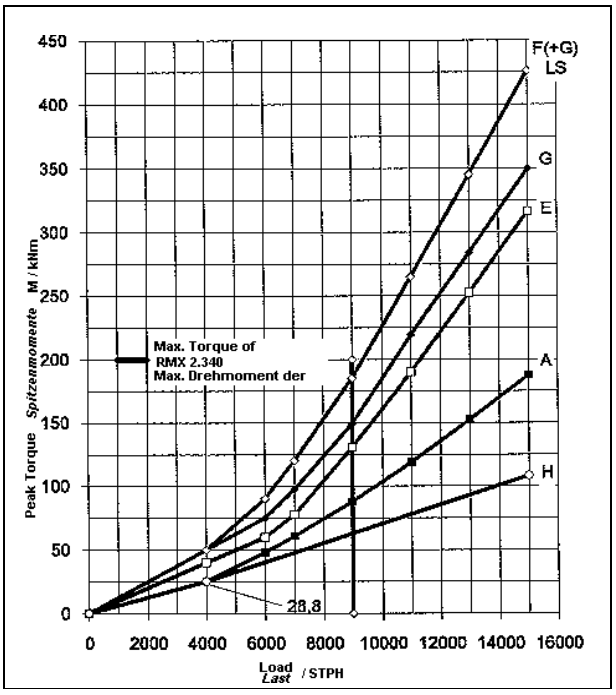

Fig.14: Dynamic peak torques ratio Mdyn/Mstat vs. load, half cycle at maximum value

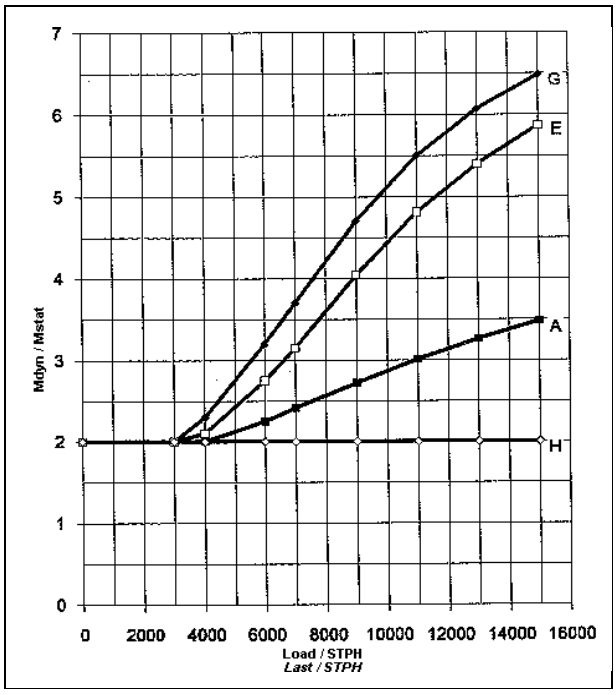

It is particularly interesting to note that as a result of the higher degree of non-linearity in curve *G*, a peak torque value emerges approximately 3.3 times that of wind-up curve *A*. This latter curve applies only to the backstop. If, instead of the elastic coupling, a stiff one (for example a diaphragm or gear coupling) had been used, this alone would have resulted in a considerable reduction in the peak torque.

Fig. 13 shows, in conciusion, the maximum dynamic peaktorques at the backstop after a half-oscillation, depending on the conveyor belt load in STPH. It is possible to see from this diagram what maximum load is allowed on the conveyor plant assuming a maximum torque of 200 kNm at the back-stop. The maximum load for curve *G* is 10,500 STPH, for curve E 11,300 STPH , and for curve *A* 15,500 STPH.

The results of Fig. 13 have been compiled in Fig. 14 in such a way that only the wind-up M_{dyn}/M_{stat} for the various ratio curves depending on the load capacity in STPH are given. One can clearly see that when the coupling elasticities (curve *G*) are taken into account, a load of 15,000 STPH achieves a peak torque 6.5 times that of the static torque.

6. Calculation Results for Unequal Load Sharing

6.1 Combination of Wind-Up Curves and Torque-Time-Functions

Many attempts have been made in the past to find suitable load sharing mechanisms for the backstops in multiple drive conveyor plants. Such mechanisms are meant to ensure a uniform load at each backstop. Unfortunately, most of these mechanisms have not been successful. One exception is described in [8]; it is a friction type torque limiter which ensures sufficiently wide angular movements in order to distribute the load. However, this system can only be built for relatively small torques. In Section 5 the assumption is made for the calculations that during the stopping process the torque is distributed identically on both backstops at the head pulley, In the cases *C, E* and *G* it was assumed that in the beginning of the stopping process the torque arms of both backstops are at the equal clearance *CL* from the first contact to the springs used for load sharing.

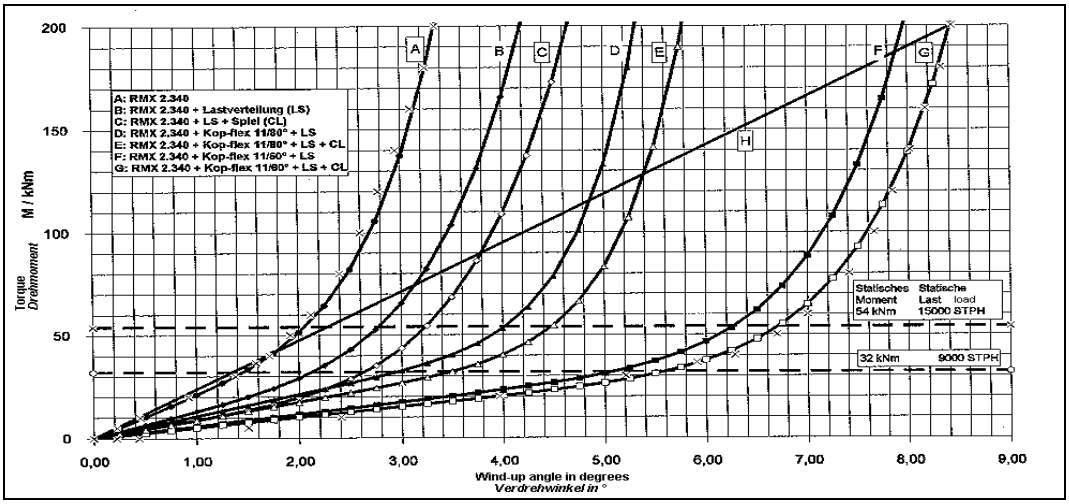

Fig.15: Wind-up characteristics in a conveyor drive at backstops shaft, load sharing

In this section it is now assumed that at the beginning of the stopping process the torque arm of only one of the backstops is located with zero load on the springs. In Fig. 15 the wind-up curves for this case are marked with *B, D* and *F*. The torque arm of the other backstop shall be at a distance *CL* from
the springs (as supposed in Section 5). For this backstop the wind-up curves *C, E* and *G* apply.

The dynamic calculations were made in such a way that the corresponding wind-up curves combined and became one. This was made by producing the sum of torques for equal torsional angles and by calculating a new function on this basis, according to Eq. (7). After these calculations the torque for each torsional angle, corresponding with each backstop, was determined, using the two curves *B* and *C,* or *F* and *G,* or *D* and *E.*

Fig.16: Dynamic torque vs. time, first half backstopping cycle backstop shaft, load sharing.

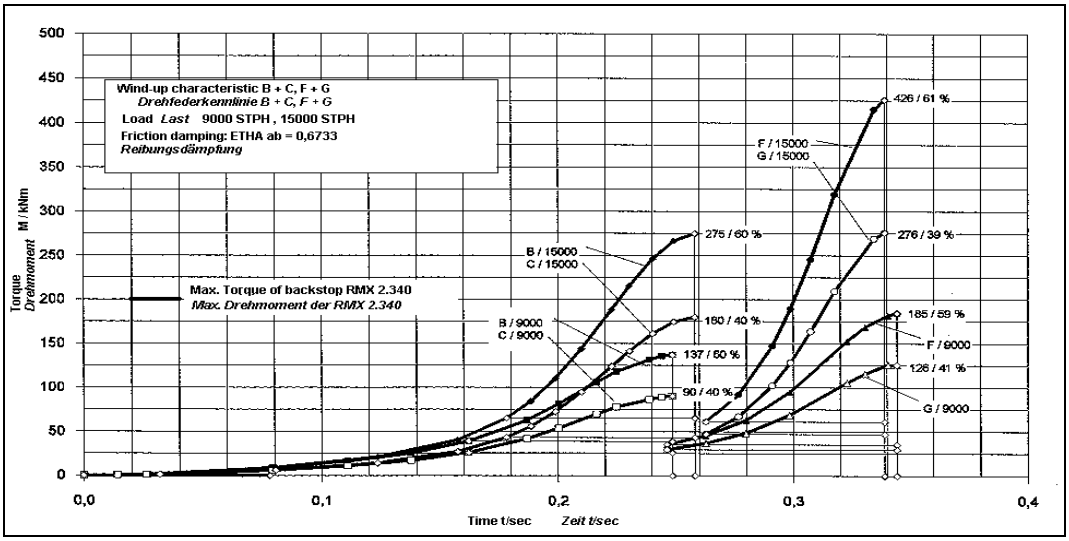

The results of these calculations can be found in Fig. 16 for the curves *B* and *C* as well as *F* and *G* for the load conditions 9, 000 and 15,000 STPH. In the case of 15,000 STPH and the curves *F* and *G*, for example, the load distribution is 61% / 39%, i.e., the backstop with curve *F* takes 426 kNm (= 61 %), and backstop *G* takes 276 kNm (= 39%). So the backstop *F* must carry a much higher torque than in the symmetrical case of 350 kNm (see Fig. 12, curve *G*). Thus it can be seen that the springs do not achieve any considerable reduction in load sharing.

6.2 Peak Torque and Load Distribution of Tension in One Gear Unit

The previous paragraph has already shown clearly that clearance can create greatly different peak torques in the backstops. The load sharing becomes even more uneven when one motor stops before the other. In the idle unit a total relaxation of the individual elements, i.e. the coupling and the gears, will occur while the plant is still running. In the second drive unit the rotating masses cause the state of tension between the gears and coupling elements to remain. When the conveyor belt reaches the velocity = 0, the torsionally flexible coupling is in tension and the reverse movement starts. In this unit a torsional angle already exists, whereas the other unit starts in the \Wind-up curve from zero.

The varjous wind-up curves in Fig. 17 have been calculated under the assumption that in one of the two gear units half of the static load of 16 kNm is still effective.

Fig.17: Wind-up characteristics in a conveyor drive, backstop shaft, load sharing and preload in one drive

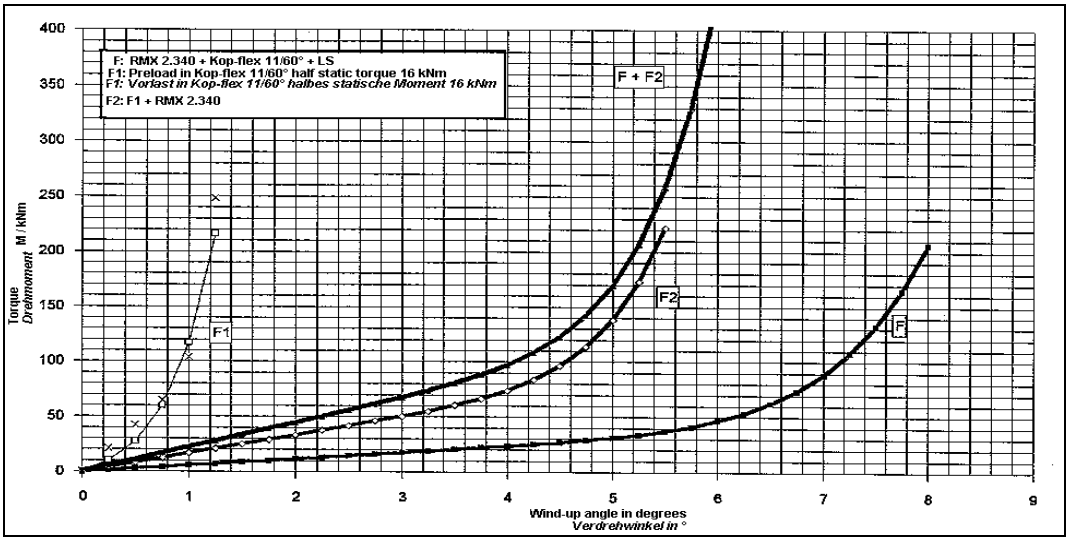

Fig.18: Dynamic torque vs. time, first half backstopping cycle, load sharing and preload in one drive, backstop shaft

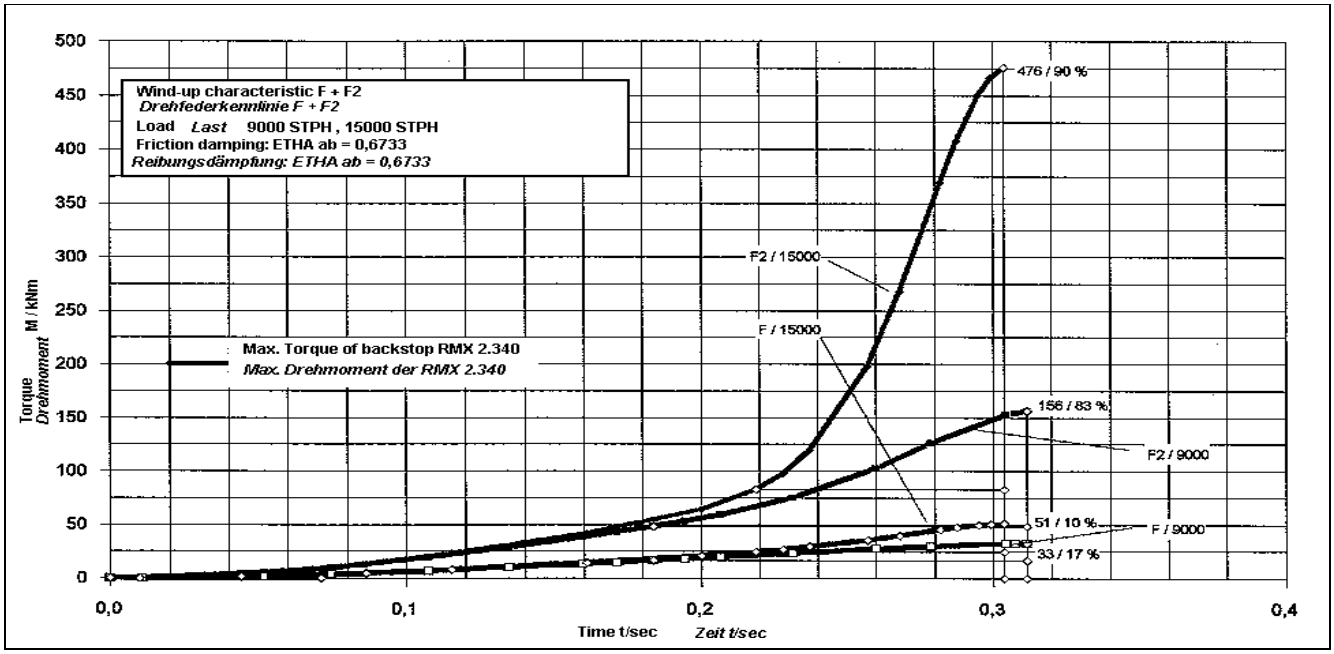

Fig. 18 shows the torque-time function for the two load conditions 9,000 and 15,000 STPH. Here it is obvious how inadequately the load distribution works under these conditions. With the load of 15,000 STPH one backstop has to take 90%, that is 476 kNm, whereas the other backstop only takes 10% or 51 kNm. This proves that under the extreme conditions the whole load will have to be taken by only one backstop.The demand referred to in [3] is completely justified, i.e., that backstops have to be designed to be able to take the full load if there is no effective device assuring load sharing.

7. Conciusions for the Selection of Backstops in Conveyor Plants

It has been thoroughly described in this paper that peak torques many times higher than the static reverse torques can occur in backstops of conveyor plants. Many calculation methods that have been used are not correct for certain cases and lead to undersizing the backstops. The method according to [8] has proved the best.

For the selection of conveyor drive components between backstop and pulley it should be kept in mind that they should have the highest possible stiffness with torsionally linear curves. Rubber element couplings between the conveyor pulley and the backstop are not recommended. Load sharing mechanisms with springs and clearances are also unsuitable. The torque arm of the backstop should either be in a horizontal position, so that its own weight eliminates the clearance as much as possible or, a spring preload should be used with the torque arm in the stopping direction to establish contact with the foundation.

If there is any doubt about the correct selection it is advisable to carry out dynamic torque calculations and to seek the advice of experts.

References

[1] ALLES, R.: Transportband-Fördergurtberechnungen; Edition Contitec Hannover, 3rd Edition, 1991.

[2] VIERLING, A.: Zur Theorie der Bandförderung; Transportbanddienst 8, 4th Edition, 1987, Contitec Hannover.

[3] NORDELL, L.K.: The Channar 20 km Overland; bulk solids handling Vol. 1 1 (1 991) No. 4, pp. 781-792.

[4] Deutsche Norm DIN 22101, E3euth-Vedrieb 1982.

[5] Rücklaufsperren-Kataloge der Firmen:
Emerson-Morse, Ithaca NY, USA;
Formsprag-Dana, Warren MI, USA;
Marland Clutch Div., La Grange, IL, USA;
RINGSPANN GmbH, Bad Homburg, Germany;
Stieber Antriebselemente, Heidelberg, Germany.

[6] TIMTNER, K.: Berechnung der Drehfederkennlinien und zulässiger Drehmomente bei Freilaufkupplungen mit Klemmkörpern; Dissertation, Darmstadt, Germany, 1974.

[7] MAURER, R. and TIMTNER, K.: Applications, improvements in service life and advanced calculation methods of freewheeling clutches; The American Society of Mechanical Engineering, 1984 - DET 164.

[8] MAURER, R.: Berührungsfreie Rücklaufsperren für hohe Drehzahlen; VDI-Berichte Nr. 649/1987.

[9] WVERKING, T.L.: Correctly located backstops reduce downtime; Energy & Mining Journal, USA, July 1991.

[10] KLOTTER, K.: Technische Schwingungslehre; 2nd and 3rd Editions, Springer-Verlag, 1951-1978.

[11] SETO, W.W.: Mechanicai Vibrations; Schaum Publishing Company, New York, 1964.